Rotor modeling of an electric motor supported by magnetic bearings through the finite element method

Ujihara, Diogo Y., diogoujihara@yahoo.com.br
Postgraduate Program on Mechanical Engineering, Fluminense Federal University (UFF), Niterói, Brazil.

Santisteban, José A., jasantisteban@vm.uff.br
Postgraduate Program on Mechanical Engineering, Electrical Engineering Department, Fluminense Federal University (UFF), Niterói, Brazil.

Noronha, Roberto F. de, roberto_noronha@vm.uff.br
Postgraduate Program on Mechanical Engineering, Mechanical Engineering Department, Fluminense Federal University (UFF), Niterói, Brazil.

Abstract. *The rotor of an induction motor rotor is supported by active magnetic bearings. The system was tested satisfactorily aiming at studying its dynamic behavior. The displacement controllers were designed by considering that a rigid body approach was good enough to represent the mechanical model of the rotor. In the present contribution the maximum speed of rotation was 6000 rpm. As higher speeds are necessary to continue the research work, the main objective of this paper is to show how to obtain an improved model of the rotor by using the finite element method. To validate the improved model, some simulation results, related to the vibration modes of the system, are compared with experimental data.*

Keywords*: rotor dynamics, finite elements method, active magnetic bearings.*

1. INTRODUCTION

Since one decade ago, an application of magnetic bearings has been performed at Federal Fluminense University (UFF). It is about the substitution of the mechanical ball bearings of an induction motor by electromagnetic devices. This subject was motivated by one of the advantages of magnetic bearings, which is the drastic reduction of friction (Schweitzer et al., 2009). The electromechanical design of magnetic bearings was conceived in such a way that the original dimensions of the electrical machine were minimally modified (Chapetta et al., 2002), (Santisteban et al., 2004). Fig. 1 shows the actual picture of the prototype under study and in Fig. 2, the details of the covers and rotors are shown.

As known, in order to hold the rotor suspended around an equilibrium position, without mechanical contact with the stator, two approaches of control systems can be designed. The first one considers the mechanical system decoupled, so that SISO (single input - single output) conventional controllers may be used, by instance PD (proportional derivative) or PID (proportional integral derivative) controllers. In the second case, the mechanical system is considered as a MIMO type (multiple input – multiple output) thus, with a state-space modeling, a feedback matrix can be designed (Schweitzer et al., 2009), (Ogata, 2003).

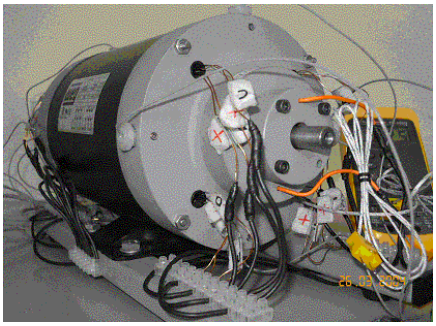

Figure 1. Prototype of an induction motor with magnetic bearings.

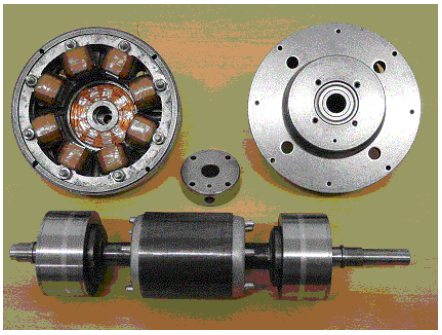

Figure 2. Details of the rotor, covers and the stator of magnetic bearings.

Some works, using the prototype, related to these approaches have been reported in Rodrigues and Santisteban (2006) and Velandia et al. (2005). In both cases, the mechanical model was implemented considering the rotor as a rigid body. This was acceptable while the maximum rotor speed was 6000 rpm, below of the first critical frequency, as will be shown. However, expecting higher speeds, an improved model is necessary.

This goal can be achieved by different approaches, including experimental ones. In this work, considering the different parameters of the rotor and taking the Finite Element Method (FEM) as a tool, a specific program was developed. The mechanical model, obtained with this program, was validated through experimental measurements.

In the following, the fundamental equations of the classical modeling of the rotor, as a rigid body and as flexible one, will be shown.

2. MODELING OF THE ROTOR AS A RIGID BODY

A conventional modeling of the rotor as a rigid body is presented in several references, by instance, in Schweitzer et al. (2009) and Rodrigues and Santisteban (2006). Fig. 3 depicts a rotor suspended by active magnetic bearings (AMB´s), where the displacements of the center of mass and the rotor sections which are submitted to the magnetic forces, are indicated.

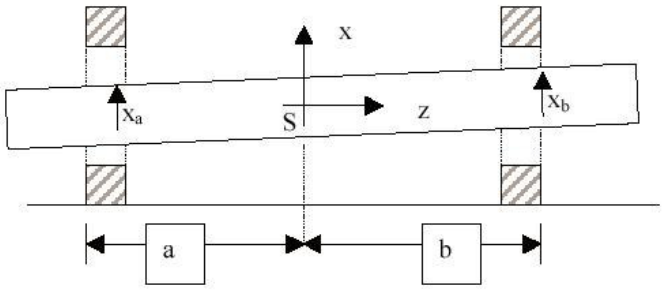

Figure 3. A rigid rotor suspended by AMB´s.

According to this approach, the rotor modeling is described by the following equations:

$$\mathbf{M_B}\ddot{\mathbf{z}}_\mathbf{B} + \mathbf{G_B}\dot{\mathbf{z}}_\mathbf{B} = \mathbf{f_B} \tag{1}$$

where:

$$\mathbf{z_B} = [x_a \quad x_b \quad y_a \quad y_b]^T \tag{2}$$

$$\mathbf{f_b} = [f_{ax} \quad f_{bx} \quad f_{ay} \quad f_{by}]^T \tag{3}$$

And $\mathbf{z_B}$ is formed by the radial displacements of the rotor caused by the applied magnetic forces. The matrices $\mathbf{M_B}$ and $\mathbf{G_B}$ are obtained as follows:

$$\mathbf{M_B} = \mathbf{T_B^T M T_B} \tag{4}$$

$$\mathbf{G_B} = \mathbf{T_B^T G T_B} \tag{5}$$

Where, **M** and **G** are obtained taking into account the mass of the rotor, the inertias and the rotation speed. $\mathbf{T_B}$ is a matrix used to transform the coordinates of the center of mass to the coordinates of the bearings.

After some manipulation, Eq. (1) is transformed to Eq. (6) and, defining $\mathbf{M_G}=\mathbf{M}^{-1}\mathbf{G_B}$ and $\mathbf{M_{bi}}=\mathbf{M_b}^{-1}$, the block diagram shown in Fig. 4 can be constructed.

$$\ddot{\mathbf{z}}_\mathbf{B}=\mathbf{M}_\mathbf{B}^{-1}\mathbf{G}_\mathbf{B}\dot{\mathbf{z}}_\mathbf{B}+\mathbf{M}_\mathbf{B}^{-1}\mathbf{f}_\mathbf{B} \tag{6}$$

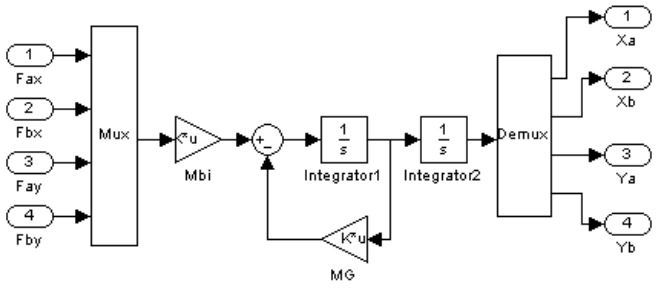

Figure 4. Block diagram of the rotor model using the rigid body approach.

3. MODELING OF THE ROTOR AS A FLEXIBLE BODY

The modeling of a flexible rotor, using the FEM, may be found in different references as in Lalanne and Ferraris (1998), Shuliang and Palazzolo (2008) and Schweitzer et al. (2009).

In this work, the elements: disk and beam, were considered. The bearing element was not considered because when AMB´s are used, the equivalent stiffness and damping are established by the parameters of the closed loop control of the radial displacements. In this case, the inputs to the model are the magnetic forces and the outputs are the radial displacements. It is from this mechanical model that the displacement controllers are designed.

One example of coordinates definition, according to the FEM, associated to three consecutive nodes, is shown in Fig. 5. In respect to the prototype, Fig. 6 shows the adopted distribution of nodes along the actual rotor. In each rotor of the magnetic bearing 4 nodes are considered, while in the cage rotor of the induction motor, 5 nodes are considered.

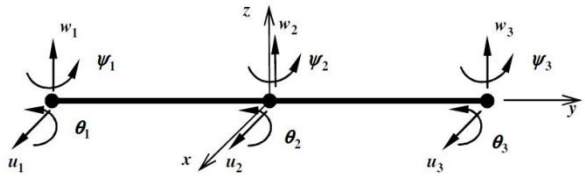

Figure 5. Coordinates of nodes.

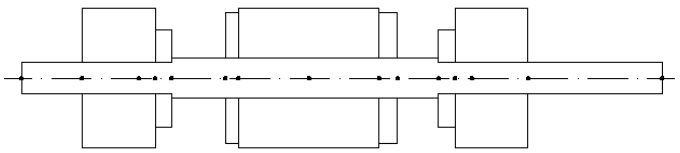

Figure 6. Distribution of nodes in the rotor.

3.1. Disk Element

According to Lalanne and Ferraris (1998), four degrees of freedom, at a given node, are considered: two displacements u and w, and two slopes θ and ψ, about the X and Z axes respectively. These can be grouped in a nodal displacement vector as:

$$\boldsymbol{\delta}=[u \quad w \quad \theta \quad \psi]^T \tag{7}$$

The application of Lagrange`s equations to the kinetic energy of the disk gives:

$$\frac{\mathrm{d}}{\mathrm{d}t}\left(\frac{\partial T}{\partial \dot{\boldsymbol{\delta}}}\right)-\frac{\partial T}{\partial \boldsymbol{\delta}}=\begin{bmatrix} M_D & 0 & 0 & 0 \\ 0 & M_D & 0 & 0 \\ 0 & 0 & I_{Dx} & 0 \\ 0 & 0 & 0 & I_{Dx} \end{bmatrix}\begin{bmatrix} \ddot{u} \\ \ddot{w} \\ \ddot{\theta} \\ \ddot{\psi} \end{bmatrix}+\Omega\begin{bmatrix} 0 & 0 & 0 & 0 \\ 0 & 0 & 0 & 0 \\ 0 & 0 & 0 & -I_{Dy} \\ 0 & 0 & I_{Dy} & 0 \end{bmatrix}\begin{bmatrix} \dot{u} \\ \dot{w} \\ \dot{\theta} \\ \dot{\psi} \end{bmatrix} \tag{8}$$

From this equation, the first matrix, denoted as $\mathbf{M_{dk}}$, is the mass matrix, and the second one is the gyroscopic matrix $\mathbf{G_d}$. Both matrices are used in the FEM program developed in this work.

3.2. Beam Element

The shaft is modeled as a beam with a constant circular cross-section. In this case, the finite element has two nodes, thus the corresponding nodal displacement vector $\boldsymbol{\delta}$ is of eighth-order, as shown below.

$$\boldsymbol{\delta}=[u_1 \quad w_1 \quad \theta_1 \quad \psi_1 \quad u_2 \quad w_2 \quad \theta_2 \quad \psi_2]^{\mathrm{T}} \tag{9}$$

The relationships between displacements and slopes are: $\psi=\partial u/\partial y$ and $\theta=\partial w/\partial y$.
Applying the Lagrange equation to the kinetic energy T of the beam element, one obtains:

$$\frac{\mathrm{d}}{\mathrm{d}t}\left(\frac{\partial T}{\partial \dot{\boldsymbol{\delta}}}\right)-\frac{\partial T}{\partial \boldsymbol{\delta}}=(\mathbf{M_c}+\mathbf{M_s})\ddot{\boldsymbol{\delta}}+\mathbf{G_c}\,\dot{\boldsymbol{\delta}} \tag{10}$$

where $\mathbf{M_c}$, $\mathbf{M_s}$ and $\mathbf{G_c}$ are obtained considering the mass, the rotary inertia and the gyroscopic effect. To calculate T, the equivalent displacements u and w, the displacement vectors $\boldsymbol{\delta_u}$ and $\boldsymbol{\delta_w}$, and the (typical) displacement functions $\mathbf{N_1}(y)$ and $\mathbf{N_2}(y)$, shown below, are used:

$$u=\mathbf{N_1}(y)\boldsymbol{\delta_u} \tag{11}$$

$$w=\mathbf{N_2}(y)\boldsymbol{\delta_w} \tag{12}$$

$$\boldsymbol{\delta_u}=[u_1 \quad \psi_1 \quad u_2 \quad \psi_2]^{\mathrm{T}} \tag{13}$$

$$\boldsymbol{\delta_w}=[w_1 \quad \theta_1 \quad w_2 \quad \theta_2]^{\mathrm{T}} \tag{14}$$

$$\mathbf{N_1}(y)=\left[1-\frac{3y^2}{L^2}+\frac{2y^3}{L^3};\quad -y+\frac{2y^2}{L}-\frac{y^3}{L^2};\quad \frac{3y^2}{L^2}-\frac{2y^3}{L^3};\quad \frac{y^2}{L}-\frac{y^3}{L^2}\right] \tag{15}$$

$$\mathbf{N_2}(y)=\left[1-\frac{3y^2}{L^2}+\frac{2y^3}{L^3};\quad y-\frac{2y^2}{L}+\frac{y^3}{L^2};\quad \frac{3y^2}{L^2}-\frac{2y^3}{L^3};\quad -\frac{y^2}{L}+\frac{y^3}{L^2}\right] \tag{16}$$

On the other hand, applying the Lagrange equation to the strain energy U of the beam element, one obtains:

$$\frac{\partial U}{\partial \boldsymbol{\delta}}=(\mathbf{K_C}+\mathbf{K_F})\boldsymbol{\delta} \tag{17}$$

Where U is obtained from the same variables used in the calculation of T. $\mathbf{K_C}$ and $\mathbf{K_F}$ are the elementary stiffness matrices (Lalanne and Ferraris, 1998). In this work, as no force is supposed in the axial direction, $\mathbf{K_F}$ was not used. In short, the matrices $\mathbf{M_{dk}}$, $\mathbf{G_d}$, $\mathbf{M_c}$, $\mathbf{M_s}$, $\mathbf{G_c}$ and $\mathbf{K_C}$ are used in the development of the FEM program.

After some manipulation, the equivalent matrices: global mass $\mathbf{M}$, stiffness $\mathbf{K}$ and gyroscopic $\mathbf{G}$ may be found. Thus, the mechanical system can be described by the equation below:

$$\mathbf{M}\ddot{\mathbf{z}}+\mathbf{G}\dot{\mathbf{z}}+\mathbf{K}\mathbf{z}=\mathbf{f_{AMB}} \tag{18}$$

Where **z** is the global nodal displacement vector, $\mathbf{f_{AMB}}$ is the global force vector given by:

$$\mathbf{f_{AMB}}=\mathbf{T_A^T f_B} \tag{19}$$

where $\mathbf{f_B}$ is the vector of magnetic forces supplied by the AMB´s and $\mathbf{T_A}$ is an auxiliary transformation matrix.

In order to control the mechanical system, a state-space representation can be obtained following the procedure below:

$$\begin{bmatrix}\dot{\mathbf{z}}\\ \dot{\mathbf{z}}\end{bmatrix}=\begin{bmatrix}-\mathbf{M}^{-1}\mathbf{G} & -\mathbf{M}^{-1}\mathbf{K}\\ \mathbf{I} & \mathbf{0}\end{bmatrix}\begin{bmatrix}\dot{\mathbf{z}}\\ \mathbf{z}\end{bmatrix}+\begin{bmatrix}\mathbf{M}^{-1}\mathbf{T}_A^T\\ \mathbf{0}\end{bmatrix}\mathbf{f_B} \tag{20}$$

Which can be rewritten in a compact form as:

$$\dot{\mathbf{x}}_s=\mathbf{A}_s\mathbf{x}_s+\mathbf{B}\mathbf{f_B} \tag{21}$$

And the four radial displacements can be obtained by: $\mathbf{y} = \mathbf{C}\mathbf{x_s}$, where $\mathbf{C}=[\mathbf{0}\ \mathbf{T_A}]$.

In this way, the block diagram of the mechanical model built from Eq. 21, which substitutes the one shown in Fig. 4, is shown in Fig. 7.

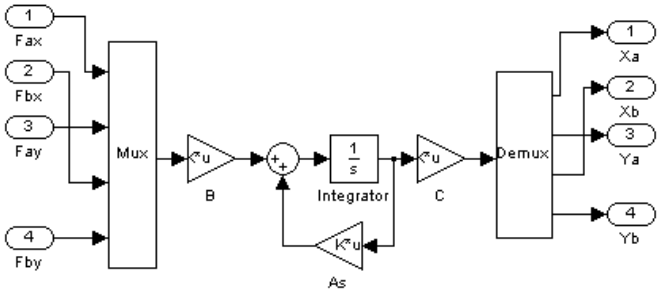

Figure 7. Block diagram of the rotor model using the flexible body approach.

4. FEM RESULTS

One program was developed in the Matlab environment (Gilat, 2006). 15 nodes were considered in the modeling of the rotor. The state space representation resulted in the assembly of one 120x120 matrix and another one of 120x 4 of size. Initially, the entire shaft was divided in beam elements and all the laminated parts of the rotors were considered as disk elements.

To validate the mechanical model obtained through the FEM, it was planned as a goal the evaluation of some vibration modes. Thus, it was executed an experiment (using a calibrated hammer), to obtain the frequency response function (FRF), shown in Fig. 8. From this, the first and second vibration modes were 536.8Hz and 1159Hz.

On the other hand, to calculate the first natural vibration modes, the eigenvalues of $\mathbf{A_s}$ were evaluated. The first simulation was unsuccessful because the respective critical vibration frequencies were far from the experimental ones. After some analysis, we found as a principal reason of this disagreement, the internal distribution of the induction motor structure. These were unknown.

In order to solve this drawback, some solutions were thought but it was found more appropriated to adapt the strategy suggested by Lalanne and Ferraris (1998) that, different to our case, it is applied to thin disks. In this way, we adopted the procedure of adjusting the diameter of the shaft, enlarging it, and the internal diameter of the disks, shortening, for both the induction motor rotor and the bearing rotors. The best result gave as vibration frequencies 587Hz and 1108Hz.

Next, using the corresponding eigenvectors of $\mathbf{A_s}$, the two first vibration modes were obtained, as shown in Figs. 9 and 10. As noted, the bending of the rotor happens in the regions where there are not disks.

Finally, ranging the speed from 0 to 1600Hz in steps of 50Hz, two Campbell diagrams were built. In both cases, an equivalent stiffness of $0.22\text{x}10^7$ N/m was used. The first one, in Fig. 11, is related to the lowest vibration frequencies for the rigid rotor model while the second one, in Fig. 12, is related to the lowest vibration frequencies for the flexible rotor model. In the speed region below 100 Hz, the vibration frequencies are similar, near to 140 Hz, which confirms the reliability of the rigid rotor model for rotation speeds below 6000 rpm.

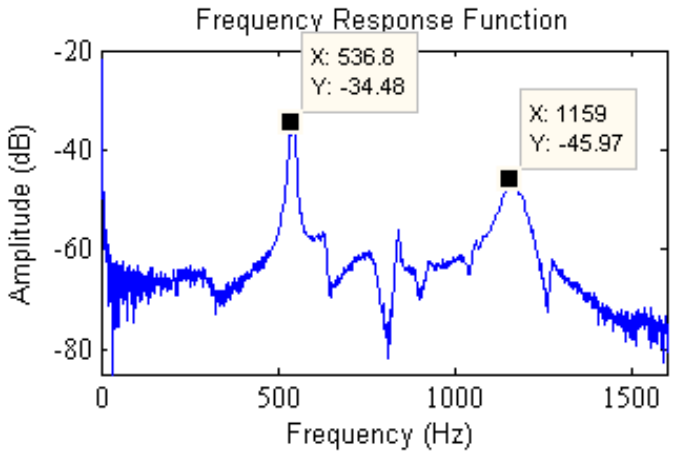

Figure 8. Experimental frequency response function (FRF) of the rotor.

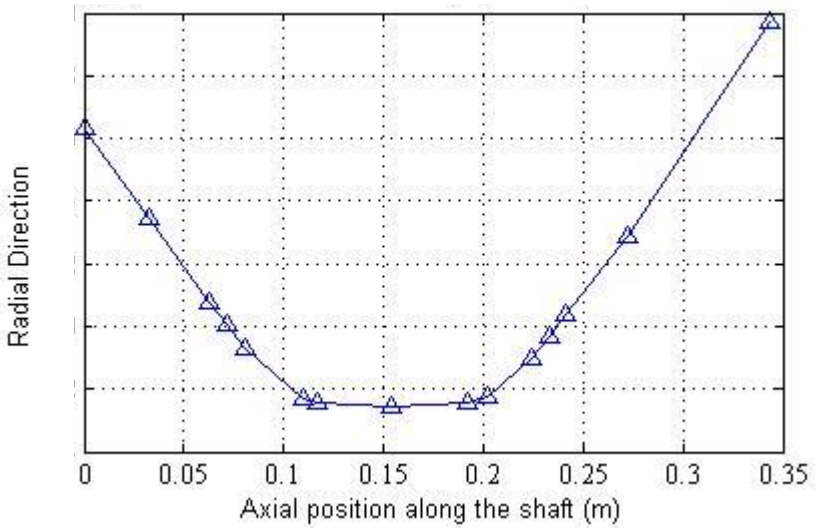

Figure 9. First mode shape using the FEM program.

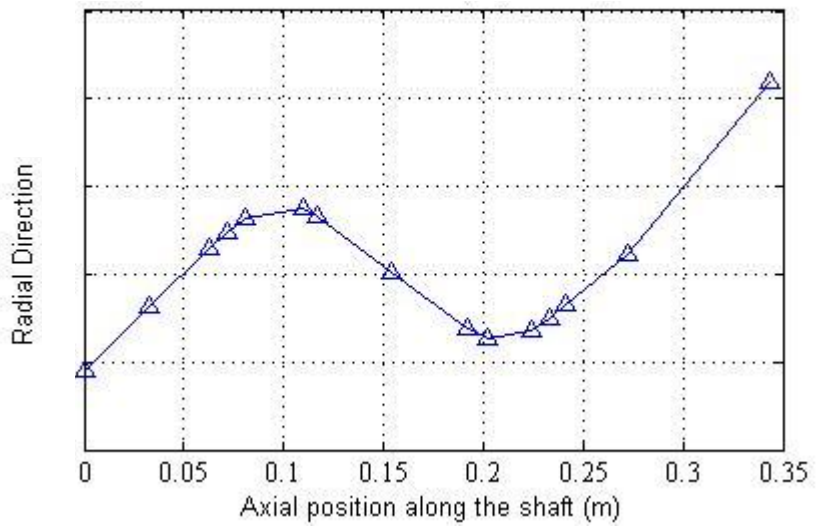

Figure 10. Second mode shape using the FEM program.

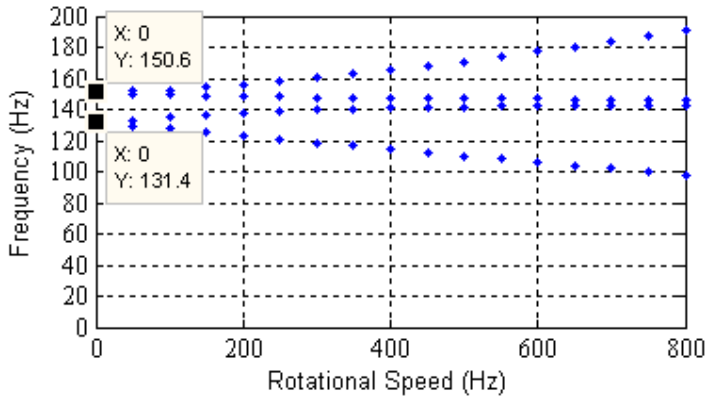

Figure 11. Campbell diagram (rigid model).

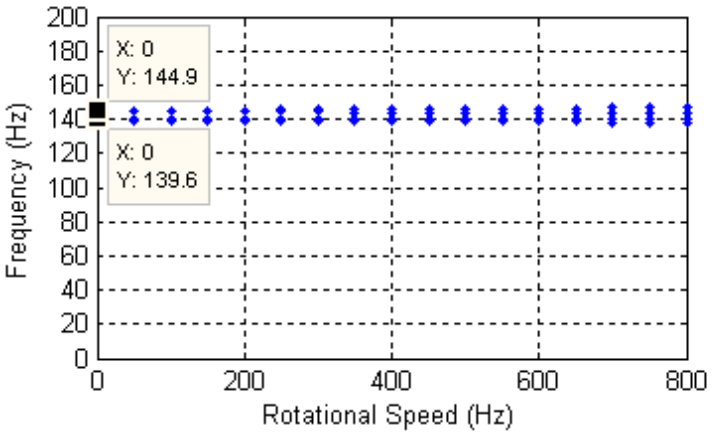

Figure 12. Campbell diagram (flexible model).

5. CONCLUSIONS

A new mechanical flexible model for a prototype of cage induction motor, supported by active magnetic bearings, was implemented using the finite elements method.

The Campbell diagrams show that, until now, the rigid body approach was enough to design the displacement controllers due to the motor operated below 100Hz.

As a next step, this new model will be used in the design of the displacement controllers for high speeds.

6. ACKNOWLEDGEMENTS

The authors gratefully acknowledge the support of CAPES.

7. REFERENCES

Chapetta, R. A., Santisteban, J. A. and Noronha, R. F., "Mancais Magnéticos – Uma Metodologia de Projeto". Congresso Nacional de Engenharia Elétrica - CONEM 2002, João Pessoa. Anais do II Congresso Nacional de Engenharia Mecânica, v. CDROM, 2002.

Gilat, A., Matlab com aplicações em engenharia. 2 ed., Porto Alegre-RS, Brasil: Bookman, 2006.

Lalanne, M. and Ferraris, G., Rotordynamics Prediction in Engineering, 2 ed., New York: John Wiley & Sons, 1998.

Ogata, K., Engenharia de Controle Moderno. 4a Edição. Rio de Janeiro: Prentice- Hall do Brasil, 2003.

Rodrigues, A. R. L. and Santisteban, J. A., "Projeto e Simulação de Controladores de Posição para um Motor Elétrico Suportado por Mancais Magnéticos". Pesquisa Naval (SDM), v. 19, p. 9-15, 2006.

Santisteban, J. A., Noronha, R. F., David, D. and Pedrosa, J. F., "Dimensionamento Mecânico, Fabricação e Montagem de um Protótipo de Motor Elétrico Suportado por Mancais Magnéticos". III Congresso Nacional de Engenharia Mecânica. CONEM 2004, Belém, Pará, 2004.

Schweitzer, G. and E. H. Maslen Editors, "Magnetic Bearings: Theory, design and application to rotating machinery". Berlin Heildelberg: Springer-Verlag, 2009.

Shuliang, L. and Palazzolo, A., "Control of flexible rotor systems with active magnetic bearings", Journal of Sound and Vibration 314, pp. 19–38, 2008.

Velandia, E. F. R., Santisteban, J. A., Noronha, R. F. and Silva, V. A. P., "Development of a Magnetically Borne Electrical Motor Prototype". COBEM 2005 - 18th International Congress of Mechanical Engineering, 2005, Ouro Preto. Proceedings of the COBEM 2005 - 18th International Congress of Mechanical Engineering. Ouro Preto : ABCM, 2005.

8. RESPONSIBILITY NOTICE

The authors are the only responsible for the printed material included in this paper.